

S263: Photometry of Star Clusters

Kanhaiya Gupta and Chelsea Maria John
Rheinische Friedrich-Wilhelms Universität Bonn.
Supervised by Maude Charmetant

March 10, 2020

The Star Clusters is a crucial object for understanding our galaxy formation and galactic stellar population as well as Big Bang theory. Numerous Globular and Open star clusters were observed through the Cassegrain telescope. The open star cluster M-34 was specifically choosen due its best seeing for the data reduction, with multiple error effects being eliminated or minimized. The age, distance from the earth and the metallicity of the open star cluster, M-34 were estimated from the best fitted isochrones and were found near to the expected values from the literatures.

Keywords: Star Clusters, HR-Diagram, Color magnitude-Diagram, Absolute magnitude, Isochrones

I. INTRODUCTION

Star Clusters form a crucial object for understanding our galaxy formation and galactic stellar population as nearly all stars in galaxies have once been member of a cluster. Since all member stars were born in a single star-brust out of one giant molecular cloud, it has a mass spectrum which can be used to study the initial mass function and thus star clusters are important tools to understand formation and evolution of population of stars with the same age, distance and metallicity.

The aim of the experiment is to derive the ages, distances and metallicities of the star clusters by comparing the observations to theoretical stellar population models of certain compositions and evolutionary stages. In our experiment a 50 cm Cassegrain reflector telescope with f-number, f/9 at its Cassegrain focus and f/3 at its primary focus is used to observe the star clusters and the Hertzsprung-Russel diagram (HRD) is used as an optimal tool for studying stellar populations and stellar evolution and their properties. The data reduction is performed using the software SKYCAT while Python is used for data analysis.

II. THEORY

A stellar cluster is a group of stars that share a common origin and are gravitationally bound for some length of time. The masses of the stars produced by the collapse of cloud fragments follow a more or less universal distribution fuction(simple power law),the so called Initial Mass Function(IMF). The IMF predicts a large number of low mass stars and a few very massive stars The canonical IMF

$\xi(m)$ has the form :

$$\begin{aligned}\xi(m) &= 0.237m^{-1.35} & m \leq M_{\odot} \\ &= 0.114m^{-2.35} & m \geq M_{\odot}\end{aligned}\quad (1)$$

The two basic categories of stellar clusters are open clusters and globular clusters.

A. Open clusters and Globular clusters

The open clusters are clusters of stars consisting of a few dozens to thousands of stars that are spread in a region with diameters in the range $1 - 10pc$. Their densities may vary from $0.1-1000M_{\odot}/pc^3$ and are asymmetrical and less centrally concentrated. Their ages range from a few million years up to about 10 billion years and are formed continuously in the galactic disks where materials can accumulate to induce star formation and have high metallicities. Some examples are the Hyades, Pleiades, M34 etc.

Whereas the globular clusters are rich clusters with 10^4-10^7 stars having diameters in the range 20 to 150pc.They are smooth and spherical with concentrated cores that extend from 0.3 to 10pc and their cores have a typical density of the order of $10^4M_{\odot}/pc^3$ Their ages are in the order of 11-13 billion years and are randomly distributed in the halo of the host galaxy and follow random orbits.The metallicity is low compared to open clusters. Globular-clusters can only form in rich molecular clouds with a high SFR(Star Formation Rate)- conditions which especially existed in the very early Universe or during the merging of two spiral galaxies. Our Milky Way has about 200 globular clusters. Prominent examples include 47 Tuc, M4, Omega Centauri, ONGC etc.

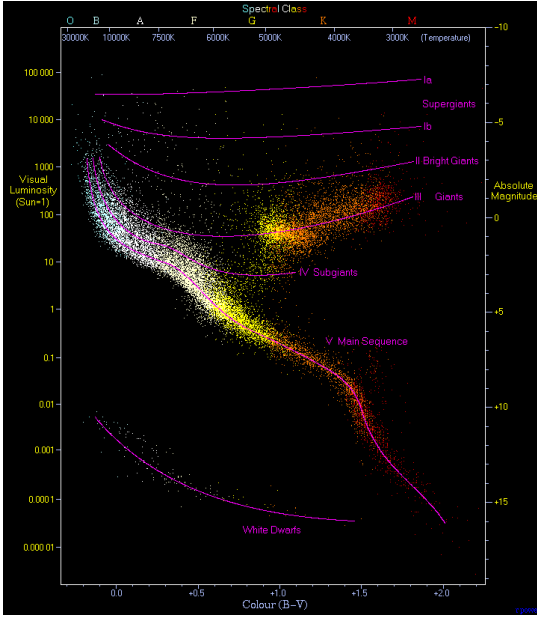


FIG. 1. A typical Hertzsprung-Russell/temperature luminosity (HRD) or color-magnitude diagram (CMD) showing 22000 stars from the Hipparcos Catalogue together with 1000 low-luminosity stars (red and white dwarfs) from the Gliese Catalogue of Nearby Stars. Valuable information on a star's evolutionary state can be derived from its position within the diagram.

Source: <http://www.atlasoftheuniverse.com/hr.html>

The two groups therefore seemed to be of completely different origin but their stellar populations, evolution and their properties can be studied accurately using Hertzsprung-Russell diagram (HRD).

B. HR Diagram & CM Diagram

The Hertzsprung-Russell diagram, abbreviated as H-R diagram, HR diagram or HRD is a scatter plot that represents a relation between the spectral classes and the absolute magnitudes of all stars. It was first presented by Henry Norris Russell at a meeting of the Royal Astronomical Society in 1913 where as Ejnar Hertzsprung anticipated the relation between the two quantities. Hitherto made efforts to replace spectral class on the abscissa by temperature and absolute magnitude on the ordinate by the star's luminosity to obtain a similar diagram: the temperature luminosity, or color-magnitude diagram (CMD).

The color-magnitude diagram (CMD) is preferred in the star photometry over H-R diagram because it is rather hard to determine the spectral class of a star, it is much easier to obtain its temperature in means of a color index. So, just by taking pictures of a star cluster with two different

filters, the temperature/color and the apparent luminosity/magnitude can be derived and a color-magnitude diagram (CMD) can be drawn. The CMD will show on its y-axis the absolute magnitude of the stars, while on the x-axis there will be the color, defined as the difference between the values of the magnitudes in the two used filters (e.g., B-V if V is on the y-axis).

The HR diagram and CMD has given a great contribution to the understanding of stellar evolution. Stars in the stable phase of hydrogen burning lie along the Main Sequence according to their mass such that higher mass at the top and lower mass at the bottom. After a star uses up all the hydrogen in its core, it leaves the main sequence and moves towards the red giant branch. The most massive stars may also become red supergiants, in the upper right corner of the diagram. The lower left corner is reserved for the white dwarfs. The useful aspects of HRD or CMD has been exploited in the experiment that determines the age of the stars clusters. The location of turn-off point, a point where some main sequence stars start deviating from their recognized patch in the diagram can be used in obtaining the age of stars in the clusters.

C. Apparent and Absolute magnitude

Measuring fluxes of celestial bodies in different frequency ranges is called astronomical photometry. The apparent magnitude, which is also called integrated radiation flux, f , m , is a measure of a star's brightness as seen by an observer on Earth and is measured in W/m^2 . Mathematically, apparent magnitude is stated as an integration of the radiation flux, f , in a specific frequency range from ν_1 to ν_2 :

$$m = \int_{\nu_1}^{\nu_2} f d\nu \quad (2)$$

The absolute magnitude M is defined as the apparent magnitude an object would have if it was located at some standard distance D , where this distance is always taken to be 10 pc. while the absolute magnitude M can be expressed from its definition as

$$m - M = 5 \log_{10}(d/D) = 5 \log_{10} d - 5 \quad (3)$$

where d is the actual length and D is the standard distance.

In order to get well defined magnitudes of star-cluster members for a color-magnitude diagram we can correct the observed fluxes of the stars by observing a reference star which is nearby the cluster and whose magnitudes in different frequency ranges/filters are well known, since the observing

conditions (air mass, filter, telescope optics, CCD) for such a reference star are approximately the same as for the cluster. By measuring f for the reference star as well as for the cluster stars and by knowing the magnitude of the reference star, we can obtain the magnitudes of the cluster stars using equation:

$$m_1 - m_2 = -2.5 \log_{10} \left(\frac{f_1}{f_2} \right) \quad (4)$$

D. Metallicities

Hydrogen and helium are the most abundant chemical element in the universe owing to their excessive formation after the Big Bang by the nucleosynthesis. So in Astronomy, all the elements other than these two are labelled as metals(M). Correspondingly, metallicity is defined as the abundance of the metals. The stars formed in the beginning (just few thousands years after the Big Bang) or in the enriched gas cloud have very low metallicities. However, the metallicities of the star increases with the time because of the nuclear fusion. Thus through stellar evolution, the metallicity in the Universe increases as hydrogen and helium are processed into heavier elements. Stars which form out of enriched material evolve differently from metal-poor stars as the metal content has a large influence on stellar evolution and the stellar structure. For instance, higher metallicities cause stars to become dimmer and cooler below a stellar mass of about $4 M_{\odot}$. Above this mass, an increase in Z only causes a decrease in a star's temperature.

Since all stars in a star cluster have the same Z , the metallicity of a cluster can be determined from a CMD by fitting various stellar-evolution models with a range of metallicities to the data and using the fact of the mass-dependent reddening and dimming of stars with increasing metallicity.

E. Cassegrain Reflector Telescope

The telescope used on the observation night is the Cassegrain reflector telescope which is mounted on the top of the Aregelander Institute for the Astronomy in Bonn. The telescope is supported on an equatorial mount which makes it capable of tracking the sky. A 50cm wide concave mirror is the main or primary mirror of the telescope. The focal length of the Cassegrain focus is 4.5m and the prime focus is at 1.5m. The Cassegrain telescopes are effective in reducing the spherical aberrations caused by the sphericity of the mirrors or lenses and therefore, making these telescopes competent in using different color filters.

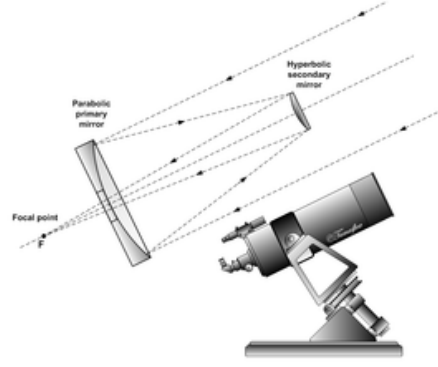


FIG. 2. Light path in a Cassegrain reflector telescope. Source: https://en.wikipedia.org/wiki/Cassegrain_reflector

The distribution of light in the image plane of an apparently point-like object is known as Point Spread function (PSF). Using the Rayleigh criterion for spatial resolution, the resolution θ of a telescope with primary aperture D is given by

$$\theta = 1.22 \frac{\lambda}{D} \quad (5)$$

where λ is the wavelength of the incoming light ray. Due to Earth's atmospheric effects like seeing and airmass, the actual resolution is much lower. In the idealised diffraction-limited case, the PSF of a circular aperture is given by the airy disc. However, due to the turbulence in the atmosphere which results in the change in the refractive index on short and temporal scales, the PSF get blurred. It is no longer an airy disc but has a more complicated shape that can be represented by a Gaussian in two dimensions. The full width at half maximum (FWHM) of this Gaussian gives the size of the stellar image, and is called the seeing of the image. The less turbulent the atmosphere, the higher resolution and thus the data quality that can be achieved.

The best observing conditions are achieved near the zenith, where the light has to travel the shortest path and is the least affected by extinction and disturbing seeing effects. The airmass tells us how much of the atmosphere light has to travel through as compared to the vertical in-fall. Higher the airmass, worse the observing conditions. \square

F. CCD Detector

The telescope uses the charged coupled device (CCD) camera to capture photons. A CCD detector consists of a two-dimensional array of picture elements (pixels), which are produced as a light sensitive metal oxide semiconductor (MOS) capacitor on a silicon substrate. CCDs make

use of the inner photoelectric effect to convert the distribution of photons to the distribution of electrons, which are then collected in capacitors and sequently read out: after an exposure is terminated, the collected charge is shifted column by column to a readout column by an alternating voltage impressed on the picture elements. The readout column is finally read out pixel-wise and the resulting signal amplified and converted to a digital signal by an analogue digital converter. CCD has lots of advantage over other photon detecting devices, such as:

- high sensitivity (high quantum efficiency of up to 90%),
- high dynamical range (the limits of luminance range that a detector can capture),
- linearity over almost the entire dynamical range,
- large spectral range (mid-infrared to ultraviolet for optical-optimised detectors),
- direct availability for further computer aided data analysis.

The major disadvantage of the CCD detectors is the production of dark currents. Picture elements (pixels) of CCD can be brought to saturation in a minute or two by the dark current at room temperature. Thus, rendering our detectors useless. To overcome it, CCD detector is cooled thermoelectrically about 30 degrees below the room temperature by using liquid nitrogen.

The CCD camera in use for the lab course is of type SBIG STL-6303E, which has 3072×2048 pixels, where the size of each pixel is $9\mu m \times 9\mu m$. It has a Full Well Capacity of $100000 e^-$, i.e. in each pixel it can store 100000 electrons, and an ADU (Analog To Digital Converter Unit) gain of $1.4 e^- / ADU$.

G. Johnson-filter system

The photometric system used in the experiment was BVR (short for blue, visual, and red) which is often called as Johnson-filter system (originally a UBV system). To measure the stellar color, the apparent magnitude of a celestial system is measured in two different spectral windows. Visual filter (V) actually is yellow-green filter owing to the tendency of human eye to observe these color more vividly. So stellar colors are measured in U-B, B-V for UVB system. And most commonly used color index is B-V which is also used in this experiment.

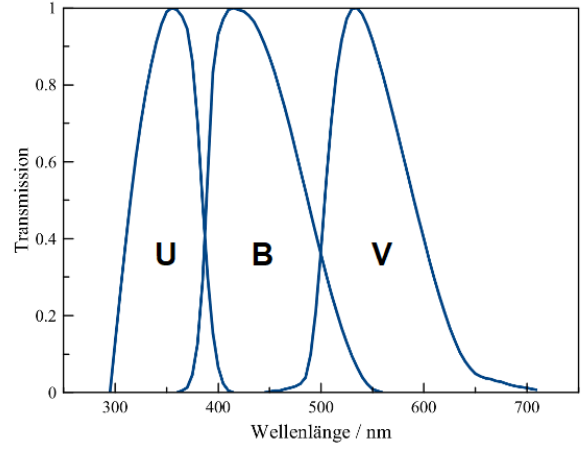


FIG. 3. UBV photometric system (Johnson-filter system).

Source: https://en.wikipedia.org/wiki/UBV_photometric_system

III. OBSERVATION

The object for night observation was preselected before the experiment night based on visibility from the <http://catserver.ing.iac.es/staralt/>. The object for observation has to be chosen with high altitude and the open cluster M34 had significant high altitude and was quite far from the moon in order to deduce signal-to-noise ratio (S/N). Before observing the astronomical objects, different frames were taken:

- 15 BIAS frames were taken for very short time considering the saturation
- 15 Dark frames were taken which accounted for creation of dark currents and cosmic rays
- 15 FLAT frames were taken for each filter (B and V) from an uniformly illuminated light source.

and finally 10 SCIENCE frames (the observation of the star clusters) were taken for two filters. The CCD detector can reach a saturation level upon long exposure time. Therefore, SCIENCE frame from bright objects were exposed for very short time whereas for fainter objects a long exposure time was needed. Also noting that long exposure time meant large signal to noise ratio (S/N). Thus, shorter exposures were made and later images were co-added. **While regardless of observation, we were provided data for reduction and analysis. We reduced and analysed the provided data.**

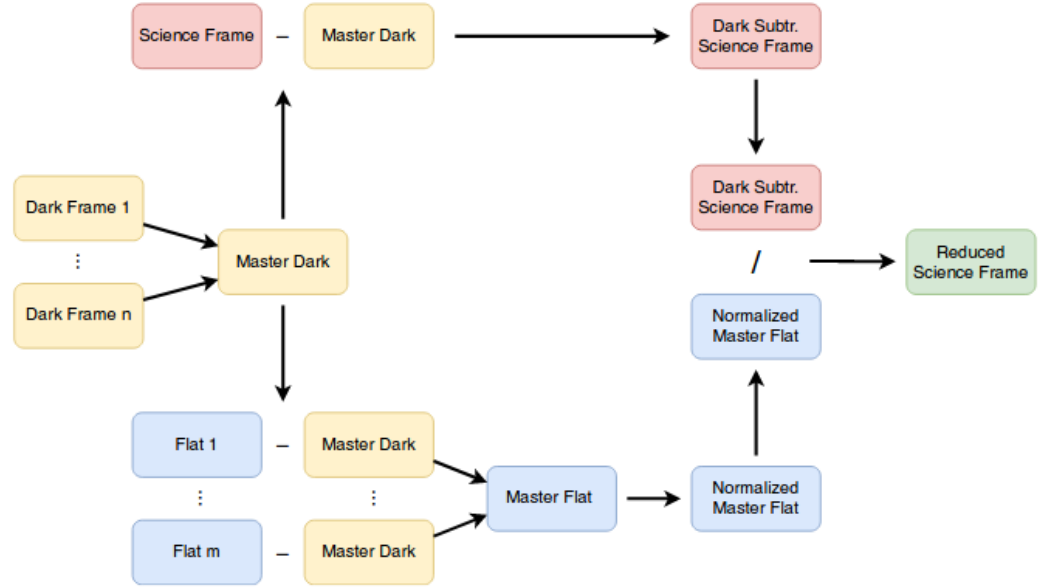


FIG. 4. A simplified scheme of the data reduction process. 1) Start by creating the master dark frame by taking the median over all n dark frames. 2) Create a master flat frame by subtracting of each flat field the master dark and then taking the median of the resulting frames. 3) The normalized master flat is derived by dividing the master flat by the mean value. 4) The final, reduced science frame is obtained by dividing the dark subtracted science frame by the normalized master flat field image

IV. DATA REDUCTION

Different sets of pictures from previous observations were processed using a software called SKYCAT in the experiment. The SCIENCE frames, which contain the information of observed star clusters, are reduced step by step.

A. Image reduction

Image reduction is done by first calibrating the observed frames and then creating a catalogue containing the magnitude of different spectrum ranges for each star in the frame and their corresponding information of position is generated. The following are the steps for image reduction:

Calibration Frames

The observed frames of the target are called as Science frames, these frames need to be calibrated in order to get a good signal to noise ratio and exclude defects of the detector, thereby making use of the data in an efficient way. The calibration is done by taking additional frames such as BIAS frames, Dark frames and Flat frames.

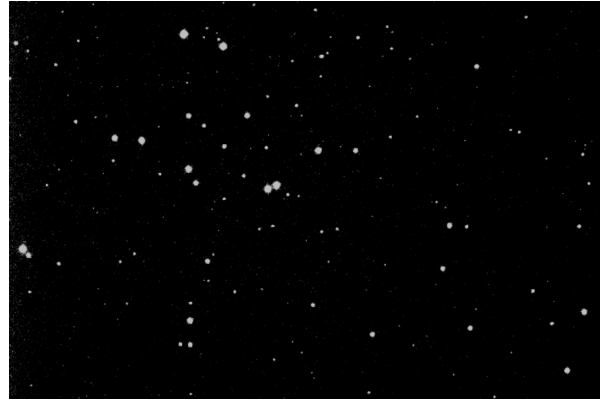


FIG. 5. Science Frame for the blue filter.

1. BIAS frames

The analog signal received from the CCD is converted to digital signal using an analog to digital converter. To get a proper scale that covers the available range of counts the logarithm of the analog signal is taken. Hence, the analog-digital converter can accept only positive values and fails for a value of zero, there by an offset is added electronically to each pixel during the read-out process before the logarithm is taken. This is called a BIAS and is obtained by taking images with zero exposure time and shutter closed. To reduce statistical errors, multiple bias frames are made and their median is taken which is further reduced from the Science

frame to get the BIAS corrected image.

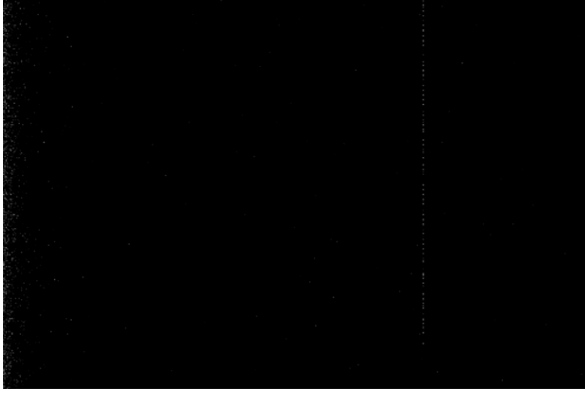


FIG. 6. BIAS frame

2. DARK frames

The CCD shows current even when it is not exposed to light due to thermal fluctuations, called as dark current. Dark current is one of the main sources of noise in image sensors such as CCD so they need to be cooled to very low temperature using liquid nitrogen to avoid saturation of pixels. The DARK frames are taken at the same temperature of the CCD and for the same exposure time as the science frames. Multiple Dark frames are taken and then their median is subtracted from the science images.



FIG. 7. Master dark frame

3. FLAT frames

FLAT frames are taken by exposing the CCD towards a uniformly illuminated background as long as the CCD reaches $\frac{1}{2}$ or $\frac{2}{3}$ saturation level. This is done in the lab with the help of a uniformly illuminated dome. FLAT images are taken to make

up for the slightly varying efficiency values of the pixels. Usually, 'donut' shapes appear in the FLAT frame which represent either dust particles in the path of the light rays or dead pixels. The pixel response is dependent on the wavelength of the incoming light, hence different frames have to be taken for each filter. During data reduction a FLAT frame will be normalized to an average value of 1 and used to divide the science image.

So far, the calibration leaves us with the reduced science frame according to this formula

$$Red.scienceframe = \frac{rawscienceframe - masterdark}{\frac{Masterflat}{\langle masterflat \rangle}} \quad (6)$$

Raw science frame is the observed science frame, master dark is the dark field obtained from combining all dark frames, master flat is the dark subtracted flat field and $\langle masterflat \rangle$ is the median value of the whole master flat field.

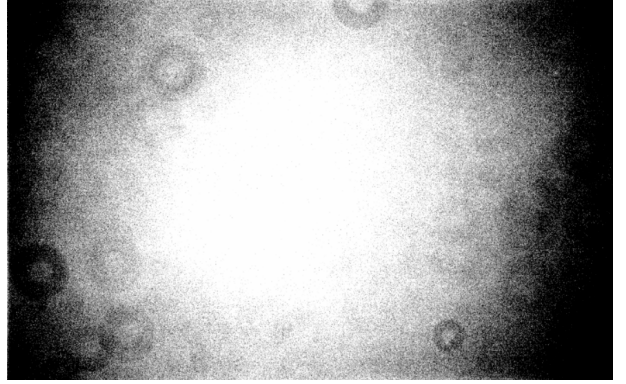


FIG. 8. Flat frame for Blue filter

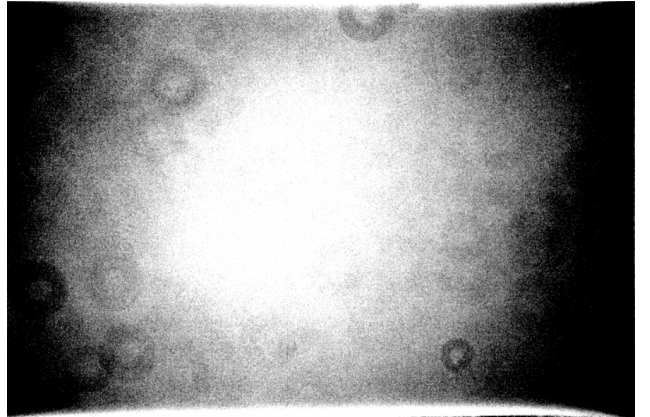


FIG. 9. Master Flat frame for B filter

B. Masking /Weighting

The defective pixels can cause problem during analysis and hence have to be masked. The masking is done by assigning different weights to the pixel like zero for dead pixels and a higher value to more sensitive pixels. The weighting factors can be taken directly from the normalised Flat frames. Weighting is necessary when you co-add frames so that a maximised S/N is obtained.

There are two types of masking – local and global. A global mask is made for a particular CCD detector and can be applied to all the imaged produced by it. In local masking individual masks for each frame is created depending on the exposure time and other factors.

C. Astrometric Calibration

To map the pixel co-ordinates to the curved sky co-ordinate astrometric calibration is required. It is done by software's with the help of reference catalogue. Here, we have used the online tool Astrometry.net

D. Sky Subtraction

The CCD collected light not only from the target but also from the background sources not in the frame like the moon. These background levels need to be removed so the flux received is only of the target in the frame. The usual way of modelling the background is to first remove all objects in your frame and then smooth the image with a specific kernel width. Then this background image can be subtracted from the original frame.

E. Co-Adding

Stacking all Science frames so that each object falls on the same pixel of the CCD, giving a higher $S \setminus N$ ration is called co-adding.

F. Photometric Calibration

Observations through different telescopes in different weather conditions results in different fluxes for the same object. Thus the apparent magnitude will be different from the true value. In order to correct this, an offset Z is added to the instrumental magnitude m_{inst} which then gives the true magnitude m_{calib} .

$$M_{cali} = m_{inst} + Z \quad (7)$$

Offsets can be calculated by observing reference stars with well known calibrated magnitudes through our instrument.

G. Cropping

After calibrating and reducing the frames the frame is cropped so that all the images taken with different filters cover the same field of view and have the same size.



FIG. 10. Reduced Science Frame for the blue filter.

V. OPEN-CLUSTER ANALYSIS: M-34 ANALYSIS

Messier-34 star cluster is an open cluster [6] with its distance to the earth equal to 470pc. The age of the cluster is 200-250 million years and metallicity $Z=0.07 \pm 0.04$. The age and metallicity is determined by fitting its colour-magnitude diagram to a certain isochrones database.

A. Magnitude Calibration

Using the SEXTRACTOR, source catalogue for the cropped final image of M-34 is created which contains the apparent magnitudes of the detected sources. To calibrate the obtained magnitudes in the catalogue for instrumental offsets, the real value of the sources are looked up in the reference catalogue (SIMBAD)[2] and the offset is calculated. On adding these offsets to the apparent magnitude we get the calibrated actual apparent magnitude of the star cluster.

$$m_{calib} = m_{instr} + \Delta m \quad (8)$$

We find for the B and V filter

$$\begin{aligned} \Delta m_V &= 1.085 \text{ mag} \\ \Delta m_B &= 0.72 \text{ mag} \end{aligned} \quad (9)$$

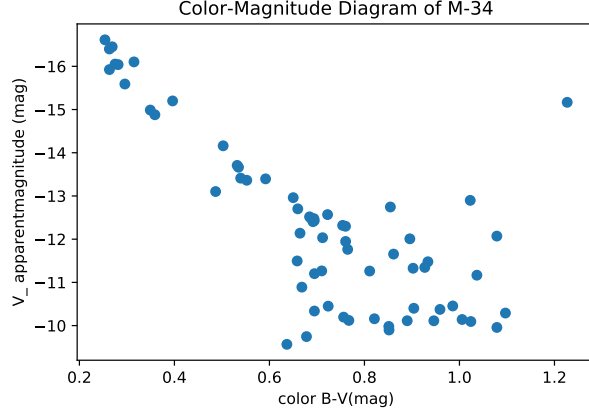


FIG. 11. Uncalibrated Color-Magnitude diagram for the Open-Cluster M-34

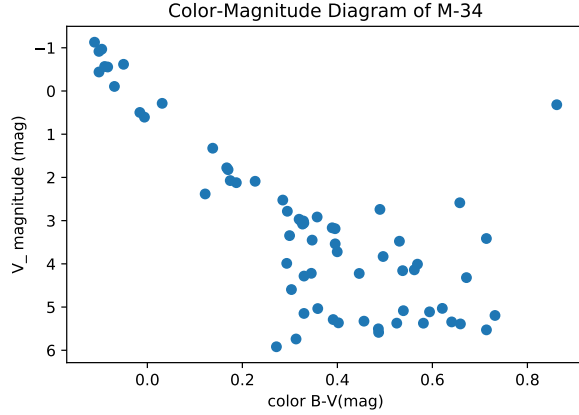


FIG. 12. Calibrated Color-Magnitude diagram for the Open-Cluster M-34

B. Extinction

The intensity of the observing stars can be decreased due to scattering in interstellar medium. Since the scattering is dependent on wavelength of the light, the factors can be determined through a colour-colour diagram in which two colour indices are plotted versus each other. This is hardly possible with the data taken from Bonn due to light pollution. Thus the extinction factor is taken as 0 for the data recorded by B and V filter.

C. Distance Determination

To determine the distance, CMD is plotted and Geneva database of isochrones is used. It contains star clusters with a set of metallicity ($Z=0.001, 0.004, 0.008, 0.020, 0.040, 0.100$). For each metallicity, there are stimulated star cluster data ranging from thousand to 15 billion years. The catalogues of these isochrones contain the absolute magnitude which is equal to apparent magnitude if measured at distance of 10 pc away from target.

In order to fit the isochrones, we need to shift out CMD plot along the y-axis. This is due to the distance modulus d , the difference between apparent and absolute magnitude. The distance modulus can be used to determine the distance to the cluster by

$$d = m - M = 5 \log_{10}(D/pc) - 5 \quad (10)$$

We find the distance modulus to have the value $d=8.4\text{mag}$. Thus the distance to M34 is calculated to be 478.63pc which is close to the literature value of 470pc.

D. Age and Metallicity determination

To determine the age and metallicity of M34, isochrones are fitted. It can be seen that the isochrones with metallicity $Z=0.04$ and $Z=0.100$ can be fitted into the whole data but for curves with low metallicity the points are away from the data. Therefore, the star clusters have metallicity in the range 0.04 - 0.10.

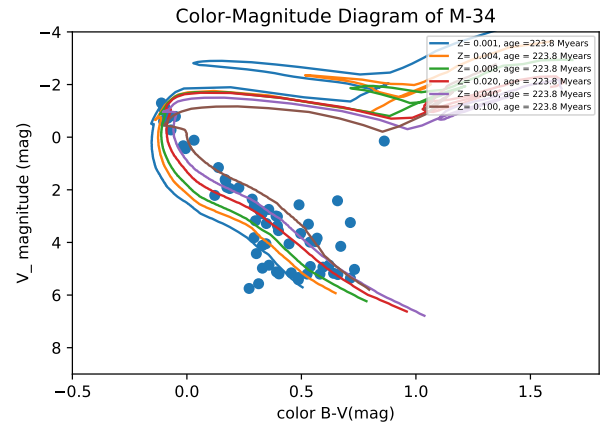


FIG. 13. A set of isochrones fitted to the color-magnitude diagram for determining metallicity of the star-cluster

To determine the age of the cluster, different isochrones having ages in the range 195 -276 Myears and metallicity 0.04 is fitted. It can be seen that curve with ages in this range is fitted nicely in the

main sequence part and RedGiant parts. Hence the age of M34 cluster is in the range 195 – 276 Myears.

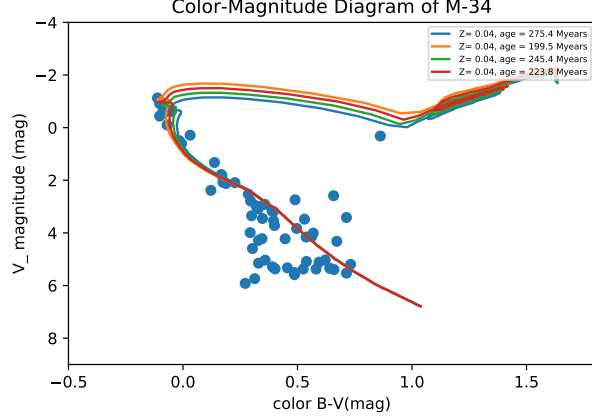


FIG. 14. A set of isochrones fitted to the color-magnitude diagram for determining the age of the star-cluster

VI. RESULTS AND DISCUSSION

In this lab, the open cluster M-34 was observed using Cassegrain reflector telescope and the data was first reduced and calibrated to minimize error and effects such as dark current, background radiation and detector inhomogeneous efficiencies. Then, Catalogue of M34 was generated using SEXTRACTOR and Color-magnitude Diagram was plotted and calibrated.

Based on the isochrone fitting to our data on the color-magnitude diagram, the age metallicity and the distance from the earth were approximated to be 195-276 million years, $Z = 0.04-0.10$ and 478.63

pc respectively.

VII. CONCLUSIONS

The experimentally obtained values for the age, metallicity and distance from the earth of the Open star-cluster M34 were obtained as 195-276 million years, $Z = 0.04-0.10$ and 478.63 pc which were quite near to the expected from the literature as 200-250 million years, $Z = +0.07 \pm 0.04$ and 470 pc.

The measured value here possesses systematical and statistical errors as well as human judgement errors. The errors in the values can be due to excluding the extinction factor, offset of the order of one in the V-filters and detector inefficiencies. The absolute magnitude calibration of V-filter by isochrone-fitting is not precise since it is done by our judgement. The fitting of the isochrones is also not very effective way to determine ages of old clusters and might be better for younger clusters.

The main sequence is not a thin line and is spread out but the numerical simulation have well defined parameters hence the fitting won't be exact. The clusters though said to be homogenous might have different metallicities because of inhomogeneities in the molecular cloud. Uncertainties can be reduced by local calibrations. And the analysis of the data were performed for the six science frames which may result in the statistical errors.

VIII. ACKNOWLEDGMENTS

We wish to acknowledge Maude Charmetan, Angie Veronica and Jakob Sebastiaan den Brok for their helpful guidelines and discussion during data reduction and its analysis.

-
- [1] Advanced Lab Course, Photometry of Star Clusters Lab Manual, 2020
<https://uni-bonn.sciebo.de/>
 - [2] SIMBAD Astronomical Database-CDS(Strasbourg)
<http://simbad.u-strasbg.fr/simbad/sim-fid>
 - [3] Atlas of the Universe
<http://www.atlasoftheuniverse.com/hr.html>
 - [4] Wikipedia, Cassegrain reflector telescope
https://en.wikipedia.org/wiki/Cassegrain_reflector
 - [5] Wikipedia, Johnson Filter system
https://en.wikipedia.org/wiki/UBV_photometric_system
 - [6] Wikipedia, Open star Cluster, Messier 34
https://en.wikipedia.org/wiki/Messier_34
 - [7] Skycat Tool
<http://www.eso.org/sci/observing/tools/skycat.html>
 - [8] Photometric Calibration
<http://slittlefair.staff.shef.ac.uk/teaching/>
 - [9] A catalogue for the Astronomical image
<http://www.astromatic.net/software/sextractor>
 - [10] Kroupa, Pavel, et al. "The stellar and sub-stellar IMF of simple and composite populations." arXiv preprint arXiv:1112.3340, 2011.
 - [11] Koçak, Dolunay, Tuğçe İçli, and Kadri Yakut. "Photometric study of close binary stars in the M35, M67, and M71 Galactic clusters." arXiv preprint arXiv:2002.05159, 2020.

APPENDIX

Preparatory Tasks

T2.1:

For stars with mass less than $0.5M_{\odot}$, we have the function

$$\xi(m) = 0.237m^{-1.35}$$

. Integrating this from $0.08M_{\odot}$ to $0.5M_{\odot}$,

$$\frac{N_{m \leq 0.5M_{\odot}}}{N_{tot}} = \int_{0.08M_{\odot}}^{0.5M_{\odot}} 0.237m^{-1.35} dm$$

$$\Rightarrow \frac{0.237}{-0.35} [0.5^{-0.35} - 0.08^{-0.35}] = 0.776015$$

The number of stars with mass $m \leq 0.5M_{\odot}$ is

$$N_{m \leq 0.5M_{\odot}} = 0.776015 \cdot 10^6 = 776015$$

T2.2:

The binary fraction of a star cluster is defined as

$$f_{bin} = \frac{N_{bin}}{N_{bin} + N_s}$$

Given that $f_{bin} = 0.7$, and total number of observed point sources $N_{bin} + N_s = 1000$, we get the number of binary systems $N_{bin} = 700$. Since every binary system contains 2 stars, the number of stars in the binary system $2N_{bin} = 1400$ stars. The number of single stars $N_s = 1000 - 700 = 300$ stars. The total number of stars in the cluster is therefore $2N_{bin} + N_s = 1700$ stars.

T2.3:

The angular size of an object is given by

$$\theta = \frac{d}{D}$$

where d is the actual size of the object, and D is the distance between the object and the observer. The angular sizes for:

- A typical globular cluster in the halo: $d = 50$ pc, $D = 10$ kpc

$$\theta = \frac{50}{10^4} = 5 \cdot 10^{-3} rad = 17' 11''$$

- A typical open cluster in the disk: $d = 5$ pc, $D = 1$ kpc,

$$\theta = \frac{5}{10^3} = 5 \cdot 10^{-3} rad = 17' 11''$$

- The full moon; $d = 10^{-10}$ pc, $D = 10^{-11}$ kpc;

$$\theta = \frac{10^{-10}}{10^{-8}} = 10^{-2} rad = 34' 22''$$

T2.4:

For the reference star with the apparent magnitude $m_{ref} = 15.0$, we observe $f_{ref} = 16000$ counts. Then, an object for which we observe $f_{obj} = 4000$ counts, the apparent magnitude is given by

$$m_{obj} = m_{ref} - 2.5 \log_{10} \frac{f_{obj}}{f_{ref}}$$

$$\Rightarrow 15 - 2.5 \log_{10} \left(\frac{4000}{16000} \right) = 16.5$$

T2.6:

For an extinction of $A = 0.2$ mag, the distance can be found by

$$m - M = 5 \log_{10} \left(\frac{D}{pc} - 5 + A \right)$$

$$\Rightarrow D = 10^{\frac{m-M+5-A}{5}} = 10^{\frac{16.5-10+5-0.2}{5}} = 181.97 pc$$

T2.7

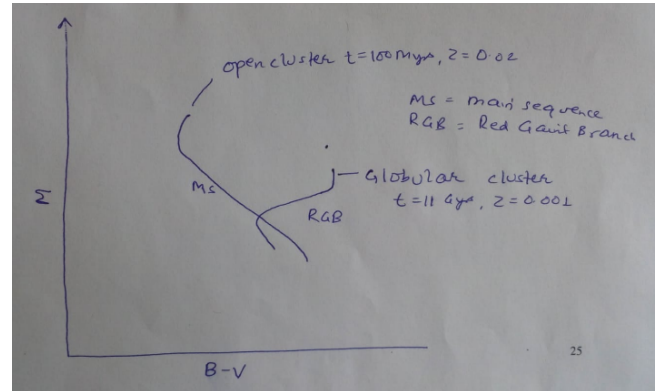


FIG. 15. CMD for an open cluster with $t = 100$ Myrs, $Z = 0.02$ and a globular cluster with $t = 11$ Gyr, $Z = 0.001$

T3.1:

The f-ratio is given by the ratio of the focal length of the system f to the diameter, D of the telescope. Here, $D = 0.5$ m

$$N = \frac{f}{D} = \frac{f}{0.5}$$

The primary focus of the telescope has an f-ratio equal to $f/3$ and the Cassegrain focus has an f-ratio equal to $f/9$.

$$\Rightarrow f_{primary} = 3 \cdot 0.5m = 1.5m$$

$$\Rightarrow f_{Cassegrain} = 9 \cdot 0.5m = 4.5m$$

T3.2:

Field of view of the telescope is given by

$$\alpha = 2 \tan^{-1} \left(\frac{d}{2f} \right)$$

where $f = 4.5 \text{ m} = 450 \text{ cm}$. For the longer side of the CCD

$$d_1 = 3072 \cdot 0.0009 = 2.8 \text{ cm}$$

$$\Rightarrow \alpha_1 = 21' 23''$$

For the shorter side of the CCD,

$$d_2 = 2048 \cdot 0.0009 \text{ cm} = 1.8 \text{ cm}$$

$$\Rightarrow \alpha_2 = 13' 45''$$

Thus the solid angle is given by $\alpha_1 \cdot \alpha_2 = 294 \text{ arc-minute}^2$. The theoretical angular resolution is given by

$$\alpha = 1.22 \frac{\lambda}{D}$$

where $D = 50 \text{ cm}$ is the diameter of the telescope. Taking $\lambda = 550 \text{ nm}$, we get $\alpha = 27.7''$. Effects such as seeing and other atmospheric effects make us unable to reach such resolutions.

T3.3:

The radians to arc-seconds conversion gives us

$$1 \text{ rad} = \frac{180}{\pi} \cdot 3600'' = 206264.8$$

The pixel size $d_p = \frac{d}{n}$, where n is the number of pixels.

$$d = n \cdot d_p = 2f \tan\left(\frac{\alpha}{2}\right) \approx f \cdot \alpha$$

$$\Rightarrow \frac{\alpha''}{n} = 206264.8 \cdot \frac{d_p / \mu\text{m}}{f / \mu\text{m}} = 206 \frac{d_p / \mu\text{m}}{f / \text{nm}}$$

T3.4:

For the standard star with $m_1 = 3.0 \text{ mag}$, the flux $f_1 = 30000/10s = 3000s^{-1}$. For a star with $m_2 = 5.0 \text{ mag}$.

$$m_1 - m_2 = -2.5 \log_{10} \frac{f_1}{f_2}$$

$$\Rightarrow f_2 = \frac{3000}{10^{0.8}} = 475.4s^{-1}$$

Thus, the exposure time $t_2 = 30000/475s^{-1} = 63.1s$.

T3.5:

The donuts in the FLAT frames are dust particles that are out of focus. From the spacing of the minima of the donut pattern, we can infer the size and the distance of the dust particle, as well as the characteristic of the telescope.

T3.6:

The full well capacity of our CCD is $10^5 e^-$, and the grain is $1.4e^-/ADU$. The maximum number of counts will thus be

$$\frac{10^5}{1.4} ADU = 71428 ADU$$

Since, FLAT frames are at $1/2$ or $2/3$ of the saturation level, we expect a count of 35714 ADU or 47618 ADU per pixel respectively. This means for a CCD of (3072×2048) pixels, we expect a total count of about $2.2 \cdot 10^{11}$ ADU or 3.10^{11} ADU respectively.

T4.1:

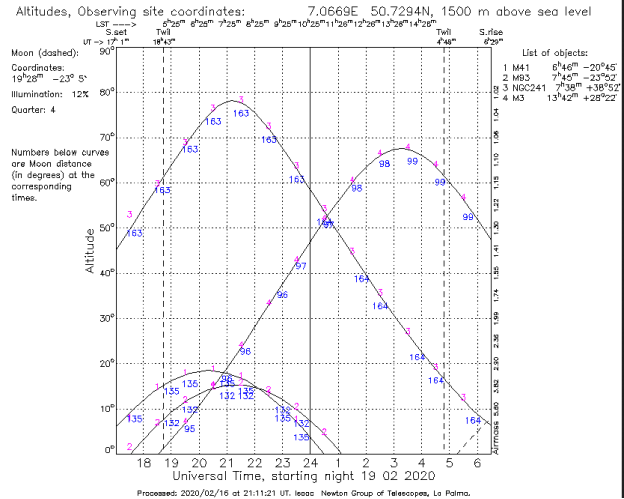


FIG. 16. Visibility plot for open and globular star cluster

T4.2:

The peak of the tracks correspond to the time when the object will be the closest to the zenith. The best open cluster to observe would be M34, and the best globular cluster to observe would be NGC 241.